

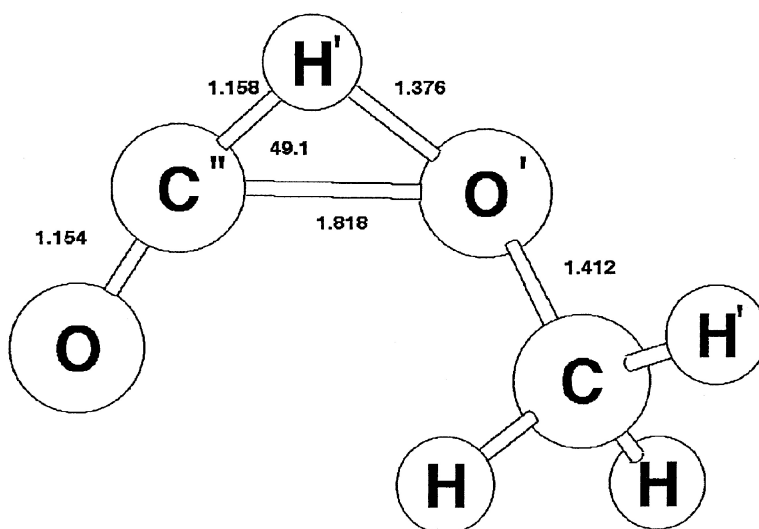
Article

## Mechanistic Study of the Gas-Phase Decomposition of Methyl Formate

Joseph S. Francisco

*J. Am. Chem. Soc.*, **2003**, 125 (34), 10475-10480 • DOI: 10.1021/ja0117682 • Publication Date (Web): 01 August 2003

Downloaded from <http://pubs.acs.org> on March 29, 2009



### More About This Article

Additional resources and features associated with this article are available within the HTML version:

- Supporting Information
- Access to high resolution figures
- Links to articles and content related to this article
- Copyright permission to reproduce figures and/or text from this article

[View the Full Text HTML](#)



**ACS Publications**  
 High quality. High impact.

## Mechanistic Study of the Gas-Phase Decomposition of Methyl Formate

Joseph S. Francisco\*

Contribution from the Department of Chemistry and Department of Earth and Atmospheric Science, Purdue University, West Lafayette, Indiana 47907-1393

Received July 20, 2001; E-mail: francisc@purdue.edu

**Abstract:** The major products of the thermal decomposition of methyl formate in the gas phase are CH<sub>3</sub>OH, CH<sub>2</sub>O, and CO. Experimental studies have proposed that the mechanism to describe these observations involves two key steps: (1) unimolecular decomposition of methyl formate to yield CH<sub>3</sub>OH + CO, followed by (2) thermal decomposition of methanol to yield CH<sub>2</sub>O + H<sub>2</sub>. The present study shows that there exists an alternative mechanism that is energetically more favorable. The new mechanism involves two competing parallel unimolecular decomposition pathways to yield the observed major products.

### I. Introduction

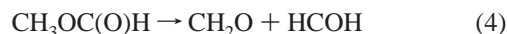
Methyl formate is the simplest member of the ester family and is a key intermediate which builds a bridge between C<sub>1</sub> molecules and diverse organic compounds.<sup>1</sup> For example, the syntheses of formic and acetic acids are based on methyl formate. Methyl formate has recently been found to be a byproduct of the oxidation of several proposed fuel alternatives, such as dimethyl ether<sup>2-4</sup> and 1,2 dimethoxyethane.<sup>5</sup> Methyl formate is well-known to be used as a precursor to syngas and has been used for syngas transport. It has also been used in the manufacture of CO in high purity from the thermal decomposition of methyl formate. There have been a number of studies that have examined the thermal decomposition of methyl formate on surfaces and with various catalysts.<sup>6-8</sup> Some recent studies have shown how doped metal oxide surfaces<sup>9</sup> and zeolites<sup>10</sup> can bring about selective decomposition of methyl formate. There have been a surprisingly large number of studies of the unimolecular decomposition studies of the methyl formate cation.<sup>11-15</sup> The intriguing issue from both an experimental and theoretical perspective is whether the underlying chemical is dominated by simple bond-breaking or molecular processes.

Despite these studies, the fundamental decomposition chemistry of gas phase methyl formate is poorly understood. In pyr-

olysis and shock tube studies,<sup>16-18</sup> the observed major products of the decomposition reaction are methanol, carbon monoxide, and formaldehyde. To describe the mechanism for methyl formate decomposition, Steacie<sup>16</sup> proposed the following mechanism



Jain and Murwaha<sup>17</sup> reported that the decomposition of methyl formate is molecular and does not involve free radical reactions. They proposed that the mechanism for methyl formate decomposition proceeds by the following steps



Shock tube studies<sup>18</sup> confirmed the mechanism proposed by Steacie<sup>16</sup> for the decomposition of methyl formate by showing the presence of CH<sub>3</sub>OH. Understanding how methyl formate decomposes is important to assessing the impact that it and its byproducts has on combustion chemistry. In the present work, the mechanisms of Steacie<sup>16</sup> and Jain and Murwaha<sup>17</sup> are examined with ab initio molecular orbital theory to determine which is energetically more favorable.

### II. Computational Methods

Ab initio molecular orbital calculations are performed using the GAUSSIAN 98 program.<sup>19</sup> The equilibrium geometry and the transition states for methyl formate are fully optimized to better than 0.001 Å for bond distance, and 0.1° for bond angles, with a self-consistent field convergence of at least 10<sup>-6</sup> on the

- (1) Lee, J. S.; Kim, J. C.; Kim, Y. G. *Appl. Catal.* **1990**, *57*, 1.
- (2) Liu, I.; Cant, N. W.; Bromly, J. H.; Barnes, F. J.; Nelson, P. F.; Haynes, B. S. *Chemosphere* **2001**, *42*, 583.
- (3) Japar, S. M.; Wallington, T. J.; Richert, J. F. O.; Ball, J. C. *Int. J. Chem. Kinet.* **1990**, *22*, 1257.
- (4) Jenkin, M. E.; Hayman, G. D.; Wallington, T. J.; Harley, M. D.; Ball, J. C.; Nielsen, O. J.; Ellerman, T. J. *Phys. Chem.* **1993**, *73*, 11 712.
- (5) Wenger, J.; Porter, E.; Collins, E.; Treacy, J.; Sidebottom, H. *Chemosphere* **1999**, *38*, 1197.
- (6) Worley, S. D.; Yates, J. T., Jr. *J. Catal.* **1977**, *48*, 395.
- (7) Barteau, M. A.; Madix, R. J. *J. Catal.* **1980**, *62*, 329.
- (8) Ushikubo, T.; Hattori, H.; Tanabe, K. *Chem. Lett.* **1984**, 649.
- (9) Ma, F.-Q.; Lu, D.-S.; Guo, Z.-Y. *J. Catal.* **1992**, *134*, 644.
- (10) Ma, F.-Q.; Lu, D.-S.; Guo, Z.-Y. *J. Mol. Catal.* **1993**, *78*, 309.
- (11) Nishimura, T.; Zhu, Q.; Meisels, G. G. *J. Chem. Phys.* **1987**, *87*, 4589.
- (12) Van Roalte, D.; Harrison, A. G. *Can. J. Chem.* **1963**, *41*, 2054.
- (13) Heinrich, N.; Schmidt, J.; Schwarz, H.; Apelois, Y. *J. Am. Chem. Soc.* **1987**, *109*, 1317.
- (14) Heinrich, N.; Drewello, T.; Burgers, P. C.; Morrow, J. C.; Schmidt, J.; Kulik, W.; Terlouw, J. K.; Schwarz, H. *J. Am. Chem. Soc.* **1992**, *114*, 3776.
- (15) Maryar, O. A.; Baer, T. *J. Phys. Chem. A* **1998**, *102*, 1682.

- (16) Steacie, E. W. R. *Proc. R. Soc. (London)* **1930**, *4127*, 314.
- (17) Jain, D. V. S.; Murwaha, B. S. *Indian J. Chem.* **1969**, *7*, 901.
- (18) Davis, C. P., Ph.D. Thesis, Graduate School of Science, University of Mississippi, Oxford, Mississippi, 1983.

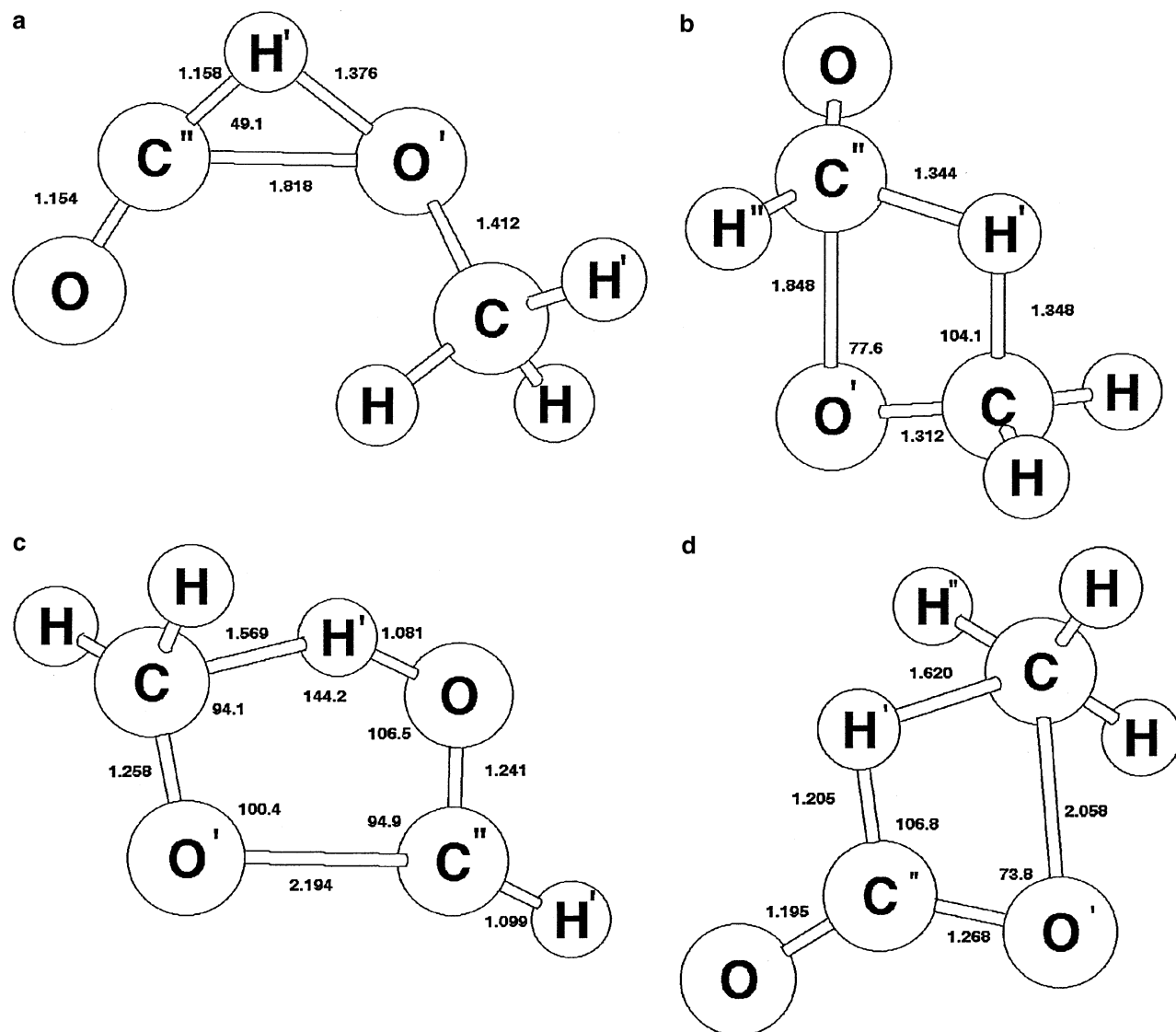


**Figure 1.** Transition States for Unimolecular Decomposition Pathways of Methyl Formate. All parameters in the Figures are taken from the MP2/6-311G-(2df,2p) geometry. A complete listing of the parameters for each transition state is given in supplementary Table 1. (a)[CH<sub>3</sub>OH + CO]<sup>‡</sup>, (b)[CH<sub>2</sub>O + CH<sub>2</sub>O]<sup>‡</sup>, (c)[HCOH + CH<sub>2</sub>O]<sup>‡</sup>, and (d)[CH<sub>4</sub> + CO<sub>2</sub>]<sup>‡</sup>.

density matrix. Initial searches for the transition state were conducted with the second-order unrestricted Møller–Plesset perturbation theory<sup>20</sup> (UMP2), with all orbitals active. We note that RMP2 wave functions are good levels of theory for close shell systems; however, when considering dissociation processes, they tend to approach the wrong dissociation limit. This is avoided in the UMP2 framework. The 6-31G(d) basis set<sup>21</sup> is used in the initial transition state searches. No restrictions on

symmetries are imposed on the initial structures, so geometry optimizations for the saddle points occurred with all degrees of freedom. The resulting structures were characterized by a harmonic vibrational<sup>9</sup> frequency analysis to confirm that a true first-order saddle point had been achieved. Vibrational frequencies were obtained with analytical second derivatives for the optimized geometries.<sup>22</sup> The Hessian from these initial searches were then used to perform optimization with the larger 6-311G-(2df,2p) basis set. Single-point energies were calculated with fourth-order Møller–Plesset theory (MP4SDTQ)<sup>23</sup> and the coupled-cluster theory [CCSD(T)]<sup>24,25</sup> with the 6-311G(2df,2p) basis set using the UMP2/6-311G(2df,2p) geometry. To evaluate the reliability of the UMP2, MP4SDTQ, and CCSD(T) calculations, several composite energy methods are also used. Methods such as G2,<sup>26,27</sup> G2MP2,<sup>26,27</sup> and CBS-Q<sup>28</sup> have been shown to

- (19) Frisch, M. J.; Trucks, G. W.; Schlegel, H. B.; Scuseria, G. E.; Robb, M. A.; Cheeseman, J. R.; Zakrzewski, V. G.; Montgomery, J. A., Jr.; Stratmann, R. E.; Burant, J. C.; Dapprich, S.; Millam, J. M.; Daniels, A. D.; Kudin, K. N.; Strain, M. C.; Farkas, O.; Tomasi, J.; Barone, V.; Cossi, M.; Cammi, R.; Bannucchi, B.; Pomelli, C.; Adamo, C.; Clifford, S.; Ochterski, J.; Petersson, G. A.; Ayala, P. Y.; Cui, Q.; Morokuma, K.; Malick, D. K.; Rabuck, A. D.; Raghavachari, K.; Foresman, J. B.; Ciwslowski, J.; Ortiz, J. V.; Baboul, A. G.; Stevanov, B. B.; Liu, G.; Liashenko, A.; Piskorz, P.; Komaromi, I.; Gomperts, R.; Martin, R. L.; Fox, D. J.; Keith, T.; Al-Laham, M. A.; Peng, C. Y.; Nanayakkara, A.; Gonzalez, C.; Challacombe, M.; Gill, P. M. W.; Johnson, B.; Chen, W.; Wong, M. W.; Andres, J. L.; Gonzalez, C.; Head-Gordon, M.; Replogle, E. S.; and Pople, J. A., GAUSSIAN 98, A.3 ed.; Gaussian, Inc.: Pittsburgh, PA, 1998.
- (20) Pople, J. A.; Jeeager, R.; Krishnan, R. *Int. J. Quantum Chem. Symp.* **1977**, *11*, 149.
- (21) Gordon, M. S.; Binkley, J. S.; Pietro, W. J.; Hehre, W. J. *J. Am. Chem. Soc.* **1982**, *104*, 2797.

- (22) Pople, J. A.; Krishnan, R.; Schlegel, H. B.; Binkley, J. S. *Int. J. Quantum Chem. Symp.* **1979**, *13*, 225.
- (23) Schlegel, H. B. *J. Chem. Phys.* **1986**, *84*, 4530.
- (24) Raghavachari, K.; Trucks, G. W.; Pople, J. A.; Head-Gordon, M. *Chem. Phys. Lett.* **1989**, *157*, 497.
- (25) Watts, J. D.; Gauss, J.; Bartlett, R. J. *J. Chem. Phys.* **1993**, *98*, 8718.

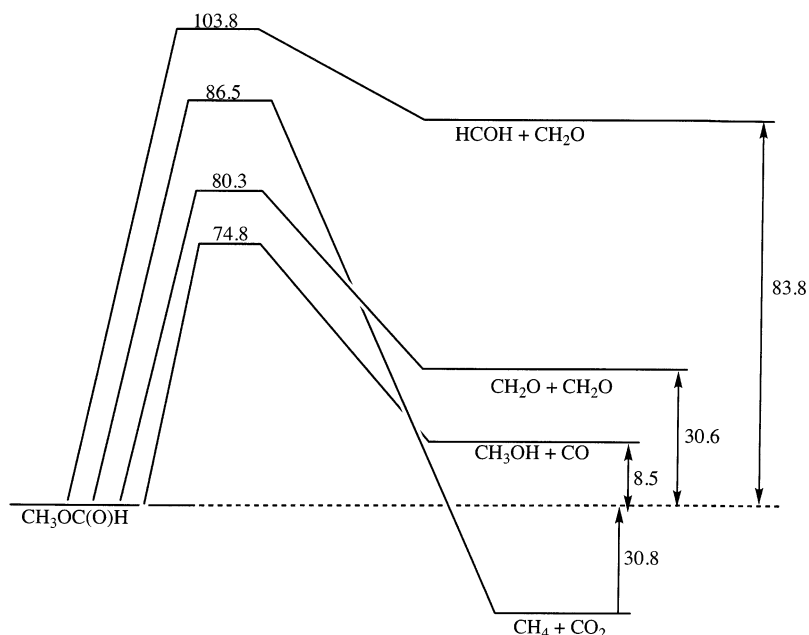


**Figure 2.** Summary of the Potential Surface for Unimolecular Decomposition Pathways of Methyl Formate. Results reported for CCSD(T)/6-311G(2df,2p)//MP2/6-311G(2df,2p) level of theory.

**Table 1.** Literature Values<sup>a</sup> for the Heats of Formation<sup>b</sup> of Methyl Formate and its Decomposition Products

species	$\Delta H_f^0$
CO	-26.4
CO <sub>2</sub>	-94.1
CH <sub>4</sub>	-16.0
CH <sub>2</sub> O	-26.8
CH <sub>3</sub> OH	-48.0
CH <sub>3</sub> OC(O)H	-85.7

<sup>a</sup> Data obtained from ref 30. <sup>b</sup> In units of kcal mol<sup>-1</sup>.

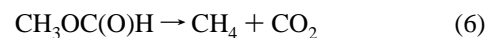
be accurate and, in general, can calculate energy differences to within 2 kcal mol<sup>-1</sup> or better. These three approaches are used in this study.

### III. Results and Discussion

The transition state for the methyl formate decomposition pathway leading to CH<sub>3</sub>OH + CO is shown in Figure 1. The geometric parameters calculated at the various levels of theory are given in Supplementary Table 1. This transition state is characterized by a three-center transition state involving the transference of the carbonyl hydrogen to the ether oxygen. Vibrational frequency calculations (Supplementary Table 2) show that the transition state is a first-order saddle point, as characterized by one imaginary frequency of magnitude 1575i cm<sup>-1</sup>.

In the experiments of Steacie<sup>16</sup> and in the shock tube studies,<sup>18</sup> one of the major products of the reaction is formaldehyde, CH<sub>2</sub>O. Most of these studies have proposed that CH<sub>2</sub>O must form from the decomposition of methanol resulting from reaction 1. However, there is an alternative route for the formation of CH<sub>2</sub>O, involving a four-center transition state shown in Figure 1b. This transition state involves the transfer

of a hydrogen from the methyl group on methyl formate to the carbonyl carbon. Vibrational frequency analysis of the 1215i cm<sup>-1</sup> imaginary frequency that characterizes this transition state shows that the molecular motion is quite complex. The major motions observed are coupling of the C''O' stretch, CH' stretch, and O'CH' bending motions. Jain and Murwaha<sup>17</sup> argued that the formaldehyde can be explained from the decomposition of methyl formate by the formation of CH<sub>2</sub>O + HCOH, reaction 4. The HCOH can then isomerize to CH<sub>2</sub>O. Jain and Murwaha<sup>17</sup> proposed on a molecular level how this transformation could take place. The transition state for this pathway has been located in this study. This transition state, shown in Figure 1c, is a five-center transition state. The transition state has been confirmed to be a true first-order saddle point, as characterized by one imaginary frequency. Its magnitude is 1098i cm<sup>-1</sup>. Steacie<sup>16</sup> reported the observation that some methyl formate is converted into methane and carbon dioxide, that is



The experiments of Jain and Murwaha<sup>17</sup> and those of shock-tube studies<sup>18</sup> did not observe these products. It is currently believed that CH<sub>4</sub> + CO<sub>2</sub> must come from secondary radical reactions. In this study, the transition state for this reaction is reported for the first time. This reaction proceeds through a late four-center transition state, shown in Figure 1d.

The total energies for the transition states, methyl formate, and the reaction decomposition products are given in Supplementary Table 3. Heats of formation values for methyl formate and its associated products from decomposition are listed in Table 1. The relative energetics for the various pathways are given in Table 2. Before the mechanistic implications of these results are discussed, it is important to look at just how reliable the energetic results are that are calculated at the various levels of theory in this study. The heat of formation of methyl formate is fairly well established, as well as those for CO, CO<sub>2</sub>, CH<sub>2</sub>O,

- (26) Curtiss, L. A.; Raghavachari, K.; Trucks, G. W.; Pople, J. A. *J. Chem. Phys.* **1991**, *94*, 7221.  
 (27) Curtiss, L. A.; Carpenter, J. E.; Raghavachari, K.; Pople, J. A. *J. Chem. Phys.* **1992**, *96*, 9030.  
 (28) Ochterski, J. W.; Petersson, G. A.; Montgomery, J. A., Jr. *J. Chem. Phys.* **1996**, *104*, 2598.

**Table 2.** Heat of Reaction<sup>a</sup> and Barrier Height<sup>a</sup> for Methyl Formate Decomposition Pathways

level of theory	CH <sub>3</sub> OH + CO		CH <sub>2</sub> O + CH <sub>2</sub> O		HCOH + CH <sub>2</sub> O		CH <sub>4</sub> + CO <sub>2</sub>	
	$\Delta H_{r,0}$	barrier height	$\Delta H_{r,0}$	barrier height	$\Delta H_{r,0}$	barrier height	$\Delta H_{r,0}$	barrier height
MP2/6-311G(2df,2p)	11.5	77.2	33.4	79.7	91.0	107.2	-33.8	89.0
MP4/6-311G(2df,2p) <sup>b</sup>	8.4	74.5	30.9	77.0	85.8	104.2	-33.6	84.2
CCSD(T)/6-311G(2df,2p) <sup>b</sup>	8.5	74.8	30.6	80.3	83.8	103.8	-30.8	86.5
G2MP2	9.8	74.7	31.5	76.7	83.8	104.1	-27.7	83.3
G2	9.3	74.2	31.3	76.6	83.5	103.8	-27.7	83.3
CBS-Q	10.6	75.1	32.2	76.6	84.8	104.0	-27.6	83.7
$\bar{X}^c$	9.7	75.1	31.7	77.8	85.5	104.5	-30.2	85.0
expt.	11.3		32.1				-24.4	

<sup>a</sup> In units of kcal mol<sup>-1</sup>. <sup>b</sup> Calculated using geometries determined at the UMP2/6-311G(2df,2p) level of theory. <sup>c</sup> Geometric mean of all six theoretical results.

**Table 3.** Total and Relative Energies for CH<sub>3</sub>OH Decomposition into CH<sub>2</sub>O + H<sub>2</sub>

method	total energies <sup>a</sup>					$\Delta H_{r,0}^b$	barrier height <sup>b</sup>
	CH <sub>3</sub> O	CH <sub>2</sub> O	H <sub>2</sub>	[CH <sub>2</sub> O + H <sub>2</sub> ] <sup>‡</sup>			
MP2/6-311G(2df,2p)	-115.54282	-114.33639	-1.16276	-115.38697	18.4	93.4	
MP4/6-311G(2df,2p) <sup>c</sup>	-115.53547	-114.32476	-1.17021	-115.38143	16.4	92.5	
CCSD(T)/6-311G(2df,2p) <sup>c</sup>	-115.53468	-114.32197	-1.17080	-115.37872	17.3	93.6	
G2MP2	-115.53182	-114.33608	-1.16636	-115.38795	18.4	90.3	
G2	-115.53490	-114.33892	-1.16636	-115.39065	18.6	90.5	
CBS-Q	-115.53828	-114.34273	-1.16609	-115.39379	18.5	90.7	
$\bar{X}^d$					17.9	91.8	
Expt.					21.2		

<sup>a</sup> In units of Hartree. <sup>b</sup> In units of kcal mol<sup>-1</sup>. <sup>c</sup> Calculated using geometries determined at the UMP2/6-311G(2df,2p) level of theory. <sup>d</sup> Geometric mean of all six theoretical results.

**Table 4.** RRKM Unimolecular Microcanonical Dissociation Rates for Methyl Formate Decomposition Pathways as a Function of Internal Energy

$E^*$ (kcal mol <sup>-1</sup> )	$k_{RRKM}(E)$			
	CH <sub>3</sub> OH + CO	CH <sub>2</sub> O + CH <sub>2</sub> O	HCOH + CH <sub>2</sub> O	CH <sub>4</sub> + CO <sub>2</sub>
80	$9.58 \times 10^5$	$1.19 \times 10^3$		
85	$1.45 \times 10^6$	$3.19 \times 10^4$		
90	$1.01 \times 10^7$	$2.73 \times 10^6$		$8.75 \times 10^3$
95	$4.57 \times 10^7$	$1.38 \times 10^6$		$1.19 \times 10^5$
100	$1.57 \times 10^8$	$5.09 \times 10^6$		$7.84 \times 10^6$
105	$4.44 \times 10^8$	$1.51 \times 10^7$	3.97	$3.44 \times 10^7$
110	$1.09 \times 10^9$	$3.82 \times 10^7$	$4.05 \times 10^2$	$1.16 \times 10^7$
115	$2.38 \times 10^9$	$8.57 \times 10^7$	$5.69 \times 10^3$	$3.26 \times 10^7$
120	$4.76 \times 10^9$	$1.75 \times 10^8$	$4.01 \times 10^4$	$7.92 \times 10^7$
125	$8.81 \times 10^9$	$3.29 \times 10^8$	$1.90 \times 10^5$	$1.73 \times 10^8$
130	$1.53 \times 10^{10}$	$5.81 \times 10^8$	$6.93 \times 10^5$	$3.47 \times 10^8$
135	$2.53 \times 10^{10}$	$9.69 \times 10^8$	$2.09 \times 10^6$	$6.44 \times 10^8$
140	$3.99 \times 10^{10}$	$1.54 \times 10^9$	$5.47 \times 10^6$	$1.13 \times 10^9$
145	$6.06 \times 10^{10}$	$2.36 \times 10^9$	$1.28 \times 10^7$	$1.87 \times 10^9$
150	$8.91 \times 10^{10}$	$3.49 \times 10^9$	$2.73 \times 10^7$	$2.97 \times 10^9$

CH<sub>4</sub>, and CH<sub>3</sub>OH.<sup>29</sup> The heats of formation are given in Table 1. A comparison of the heat of reaction for the CH<sub>3</sub>OH + CO decomposition channel, for example, show that the six various levels of theory are able to predict the energetics to within 2.4 kcal mol<sup>-1</sup> (see Table 2). The geometric mean of the six theoretical estimates is 9.7 kcal mol<sup>-1</sup> for the heat of reaction for the CH<sub>3</sub>OH + CO channel. This theoretical estimate is 1.8 kcal mol<sup>-1</sup> in error from the experimental estimate. The heat of reaction for the CH<sub>2</sub>O + CH<sub>2</sub>O channel is estimated as 31.7 kcal mol<sup>-1</sup>. Note that this is in error by 0.4 kcal mol<sup>-1</sup>. The CH<sub>4</sub> + CO<sub>2</sub> reaction gives the largest error of 5.8 kcal mol<sup>-1</sup>. This error results from the larger errors associated with the incomplete accounting of electron correlation from the MP2 and MP4 methods. These results weight the larger error between

experimental and theoretical results. Nevertheless, the rms (root-mean-square) error between experimental and theoretical heats of formation for decomposition channels of methyl formate is 4.2 kcal mol<sup>-1</sup>.

An examination of the activation energy barriers predicted by the six methods suggests that the barriers are reasonably converged. For example, with the CH<sub>3</sub>OH + CO channel, the variance between the six estimates is 1.1 kcal mol<sup>-1</sup>. For the HCOH + CH<sub>2</sub>O, CH<sub>2</sub>O + CH<sub>2</sub>O, and CH<sub>4</sub> + CO channels, the variance is 1.3, 1.7, and 2.3 kcal mol<sup>-1</sup>, respectively. These results suggest that the barriers for the MP4 and CCSD(T) results are reasonably converged. A conservative estimate of the error associated with the barriers is 4 kcal mol<sup>-1</sup>.

Presented in Table 2 are the barriers for methyl formate decomposition pathways considered in the present study. The transition state for the formation of CH<sub>3</sub>OH + CO is three-centered, as shown in Figure 1a, possessing an activation energy barrier of 74.8 kcal mol<sup>-1</sup> at the CCSD(T)/6-311G(2df,2p)//MP2/6-311G(2df,2p) level of theory. There have been three experimental studies that have reported activation barriers for methyl formate decomposition. It is interesting to note that the pathway for formic acid (HC(O)OH) dissociation into H<sub>2</sub>O + CO proceeds through a similar three-center transition state involving the transfer of a carbonyl hydrogen. Both gas phase and theoretical studies<sup>31-34</sup> show that the activation barrier ranges between 61 and 68 kcal mol<sup>-1</sup>. The ab initio predicted barrier for the CH<sub>3</sub>OH + CO methyl formate channel is reasonable. Steacie<sup>16</sup> reported an activation barrier of 48.7 kcal mol<sup>-1</sup>, Jain and Murwaha<sup>17</sup> reported a value of 47.4 kcal mol<sup>-1</sup>, and shock tube studies<sup>18</sup> reported a barrier of 50.6 kcal mol<sup>-1</sup>.

(30) Solly, R. K.; Benson, S. W. *Int. J. Chem. Kinet.* **1969**, *1*, 427.

(31) Goddard, J. D.; Yamaguchi, Y.; Schaefer, H. F. *J. Chem. Phys.* **1992**, *96*, 1158.

(32) Francisco, J. S. *J. Chem. Phys.* **1992**, *96*, 1107.

(33) Saito, K.; Kakamoto, T.; Jurado, H.; Torii, S.; Imamura, A. *J. Chem. Phys.* **1984**, *80*, 4989.

(29) Chase, M. W.; Davies, C. A.; Downey, J. R.; Frurie, D. J.; McDonald, R. A.; Syrerud, A. N. *J. Phys. Chem. Ref. Data Suppl.* **1985**.



These experimental activation barriers are 26.4, 27.7, and 24.5 kcal mol<sup>-1</sup>, respectively, lower than the theoretical barrier. Given the standard deviation between the six theoretical methods, the more than ca. 20 kcal mol<sup>-1</sup> difference between the theoretical and experimental barriers lie outside the error range of the calculations. For the CH<sub>3</sub>OH + CO channel, there may be a systematic discrepancy. Steacie<sup>16</sup> suggested that the reaction is impacted by the surface of the reaction vessel. As a result, Steacie<sup>16</sup> argued that the CH<sub>3</sub>OH + CO reaction is heterogeneous rather than homogeneous. However, shock tube studies<sup>18</sup> treated the reaction as homogeneous. The present calculated results do not support the conclusion that the barrier of activation for the homogeneous CH<sub>3</sub>OH + CO decomposition channel is 50.6 kcal mol<sup>-1</sup>. The theoretical results in Table 2 suggest that the two experimental results for the activation barriers must be influenced by surface reactions. The surface acts to catalyze the decomposition of methyl formate, of which the impact is to effectively lower the barrier. The present calculations suggest that the impact of the surface on the barrier is dramatic. Molecular beam experiments under collisional conditions could provide a better measurement of the homogeneous activation barrier for the CH<sub>3</sub>OH + CO decomposition channel. For example, the elegant molecular beam experiments of Longfellow and Lee<sup>35</sup> showed conclusively that the primary decomposition pathway for the unimolecular dissociation of acetic acid is the decarboxylation channel under collisionless conditions. These experiments resolved longstanding discrepancies in the thermal experiments in their interpretation of the mechanism and energetics for this reaction.

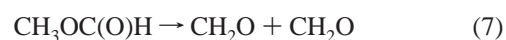
The five-center transition state for the formation of HCOH + CH<sub>2</sub>O is shown in Figure 1b, the activation energy barrier is 103.8 kcal mol<sup>-1</sup> at the CCSD(T)/6-311G(2df,2p)//MP2/6-311G(2df,2p) levels of theory, and the four-center transition state leading to the products, CH<sub>2</sub>O + CH<sub>2</sub>O, shown in Figure 1c, has an activation energy barrier of 80.3 kcal mol<sup>-1</sup> at the same level of theory. In the experiments of Steacie,<sup>16</sup> the products CH<sub>4</sub> and CO<sub>2</sub> were observed and were reported in small amounts. Jain and Murwaha<sup>17</sup> did not observe these products in their experiments. A pathway to describe the CH<sub>4</sub> + CO<sub>2</sub> products involves the decomposition of methyl formate through a four-center transition state, as shown in Figure 1d. The activation energy barrier for the CH<sub>3</sub>OC(O)H → CH<sub>4</sub> + CO<sub>2</sub> reaction is estimated as 86.5 kcal mol<sup>-1</sup> relative to the isolated products (-30.6 kcal mol<sup>-1</sup>) at the CCSD(T)/6-311G(2df,2p)//MP2/6-311G(2df,2p) level of theory. The four-center elimination pathway in dimethyl ether (CH<sub>3</sub>OCH<sub>3</sub>) to produce the products CH<sub>4</sub> + CH<sub>2</sub>O involves a similar COCH transition state.<sup>36</sup> The activation barrier for this reaction is estimated to be 89.5 kcal mol<sup>-1</sup>. The barrier for the CH<sub>4</sub> + CO<sub>2</sub> pathway is quite similar.

In the Steacie mechanism,<sup>16</sup> reaction 2 describes the formation of CH<sub>2</sub>O and H<sub>2</sub>, which are essential observable products of the methyl formate decomposition mechanism. The barrier for methanol decomposition into CH<sub>2</sub>O and H<sub>2</sub> is 93.6 kcal mol<sup>-1</sup> calculated at the CCSD(T)/6-311G(2df,2p)//MP2/6-311G(2df,2p) level of theory. The mean of this barrier calculated at the six levels of theory is 91.8 kcal mol<sup>-1</sup>, as shown in Table 3. The Steacie mechanism (i.e., reactions 1–2) involves

consecutive reaction steps. The overall energy barrier for this process is 102.1 kcal mol<sup>-1</sup> to yield the products from reactions 1 and 2.

Jain and Murwaha<sup>17</sup> proposed that the first step in the methyl formate decomposition mechanism involves the formation of HCOH + CH<sub>2</sub>O. The activation barrier for this step is 103.8 kcal mol<sup>-1</sup>. This exceeds the barrier for reaction 1 in the Steacie mechanism by 29.1 kcal mol<sup>-1</sup>. It seems unlikely that the HCOH + CH<sub>2</sub>O pathway is energetically competitive with the Steacie mechanism and seems unlikely to contribute significantly to the chemistry. The present calculations also suggest that a more plausible explanation of the observations of Jain and Murwaha<sup>17</sup> is reaction 7.

An alternative mechanism that may describe the observed products of the methyl formate decomposition reaction involves two parallel reactions that are energetically competitive, namely



The energy difference between the CH<sub>3</sub>OH + CO and CH<sub>2</sub>O + CH<sub>2</sub>O barriers is 5.5 kcal mol<sup>-1</sup>. A comparison of the overall energy barriers for the alternative mechanism suggest that it is energetically more favorable by 21.8 kcal mol<sup>-1</sup> than the Steacie mechanism<sup>16</sup> and 23.5 kcal mol<sup>-1</sup> more favorable than the Jain and Murwaha mechanism.<sup>17</sup>

It is interesting to note that the barriers for the molecular reaction steps (reactions 1 and 2) are below the energy requirement of bond fission reactions in methyl formate. Breaking the CH bond on the methyl group of methyl formate<sup>30</sup> requires ca. 100 kcal mol<sup>-1</sup> of energy, whereas the CH bond on the carbonyl group requires 92.7 kcal mol<sup>-1</sup> of energy. The CO bond fission reaction yielding CH<sub>3</sub>O + HCO requires 100.1 kcal mol<sup>-1</sup> of energy. These bond fission processes are well below the barrier for the molecular processes (CH<sub>2</sub>O + CH<sub>2</sub>O, CH<sub>4</sub> + CO<sub>2</sub>, and CH<sub>3</sub>OH + CO). Moreover, it is consistent with the observation of Jain and Murwaha<sup>17</sup> that the decomposition does not involve free radical reactions which could be initiated from bond fission processes in methyl formate. It should be noted that, if the HCOH + CH<sub>2</sub>O step is the key step as suggested by Jain and Murwaha,<sup>17</sup> CH bond fission reactions would be more competitive, and hence free-radical chain reactions would be necessary to describe the chemistry. However, this is inconsistent with the experimental observations from both static and shock tube studies that suggest no free radical reaction are involved in the mechanism. The fact that methyl formate decomposition does not give free radicals upon decomposition has important implications for its combustion chemistry, i.e., that C–C bond formation which can result from radical addition reactions is minimized. This, in turn, suggests a minimization of soot formation in combustion processes involving methyl formate.

To interpret the decomposition kinetics and assess the relative importance of the channels, energy-dependent unimolecular rates are needed. Microcanonical unimolecular rates are evaluated using RRKM theory.<sup>37,38</sup> The microcanonical unimolecular rate

(34) Blake, P. G.; Davis, H. H.; Jackson, G. *J. Chem. Soc.* **1971**, 1923.

(35) Longfellow, C. A.; Lee, Y. T. *J. Phys. Chem.* **1995**, *99*, 15 532.

(36) Nash, J. J.; Francisco, J. S. *J. Phys. Chem. A* **1998**, *102*, 236.

(37) Marcus, R. A. *J. Chem. Phys.* **1952**, *20*, 359.

constant  $k_{\text{RRKM}}(E)$ , of an isolated molecule possessing the total energy  $E$ , is given by

$$k_{\text{RRKM}}(E) = G(E-E_0)/hN(E)$$

where  $G(E-E_0)$  is the sum of states for the transition state configuration,  $N(E)$  is the density of states for the reactant, and  $h$  is Planck's constant. The input parameters used are the vibrational frequencies for the reactant and transition states given in Supplementary Table 2 (see the Supporting Information), the reduced internal moments of inertia for the reactant and transition states calculated from the optimized geometries at the UMP2/6-311G(2df,2p) level of theory, and the critical energy for each pathway given in Table 2. The results of the RRKM calculations are given in Table 4.

Over the range of 80–150 kcal mol<sup>-1</sup>, the rates for the CH<sub>3</sub>-OH + CO and CH<sub>2</sub>O + CH<sub>2</sub>O channels are competitive. At energies above 105 kcal mol<sup>-1</sup>, the HCOH + CH<sub>2</sub>O channel starts to appear. It is only at very high energies (>150 kcal mol<sup>-1</sup>), the rate constant for HCOH + CH<sub>2</sub>O becomes remotely competitive. Rates for the four-center elimination, yielding CH<sub>4</sub> + CO, are estimated to be 2 orders of magnitude slower than that for the CH<sub>3</sub>OH + CO channel at 100 kcal mol<sup>-1</sup>. At energies above 150 kcal mol<sup>-1</sup>, the CH<sub>4</sub> + CO is only 1 order of magnitude slower and becomes competitive. So, in the experiments of Steacie,<sup>16</sup> it is not unreasonable to see a small yield of CH<sub>4</sub> resulting for this channel. Consequently, the observation of CH<sub>4</sub> may result from a primary molecular decomposition channel and not from secondary free-radical chain reactions. Decomposition of CH<sub>3</sub>OH slowly comes in at threshold energies above 95 kcal mol<sup>-1</sup>. At an internal energy of 100 kcal mol<sup>-1</sup>, the CH<sub>3</sub>OH decomposition rate is  $6.8 \times 10^6$  s<sup>-1</sup>, whereas the CH<sub>3</sub>OC(O)H → CH<sub>2</sub>O + CH<sub>2</sub>O rate is  $5.1 \times$

$10^6$  s<sup>-1</sup>. This suggests that, at high energies, both the Steacie mechanism and the two competition parallel reactions could compete. At energies less than 100 kcal mol<sup>-1</sup>, for example, at an internal energy of 95.0 kcal mol<sup>-1</sup>, the methanol decomposition rate is  $8.6 \times 10^5$  s<sup>-1</sup> and the CH<sub>3</sub>OC(O)H → CH<sub>2</sub>O + CH<sub>2</sub>O rate is  $1.4 \times 10^6$  s<sup>-1</sup>. The methanol channel is slow, and below the 94 kcal mol<sup>-1</sup> threshold the channel does not have enough energy to proceed. Over the lower energy range, RRKM calculations suggest that the mechanism for decomposition of methyl formate can best be described by two competing parallel unimolecular decomposition pathways to yield the observed major products CH<sub>2</sub>O, CH<sub>3</sub>OH, and CO.

#### IV. Conclusions

An interesting question from past experimental studies of the decomposition of methyl formate is whether the observed chemistry is homogeneous or heterogeneous. The present calculations show that all the observed products can be explained by gas phase chemistry. However, the observed barriers cannot be explained by the gas phase chemistry. Only molecular beam experiments can resolve this question. Nevertheless, the present work suggests that, from a homogeneous gas phase perspective, the products from the decomposition of methyl formate can be explained by an alternative mechanism, namely with two competitive parallel reactions forming CH<sub>3</sub>OH + CO and CH<sub>2</sub>O + CH<sub>2</sub>O, followed by decomposition of CH<sub>2</sub>O, to yield CO + H<sub>2</sub>.

**Supporting Information Available:** Geometry for methyl formate transition state (Table 1S), vibrational frequencies for methyl formate and transition states (Table 2S), and total energies for reactant, products, and transition states for methyl formate decomposition pathways (Table 3S). This material is available free of charge via the Internet at <http://pubs.acs.org>.

JA0117682

(38) Robinson, P. J.; Holbrook, K. A. *Unimolecular Reactions*; Wiley-Interscience: New York, 1972.